Invited article to
Physics World

Infrared Detectors Reach New Lengths

*S. D. Gunapala, G. Sarusi, J. S. Park, T. L. Lin, and B. F. Levine**

Center for Space Microelectronics Technology, Jet Propulsion Laboratory, California Institute of Technology, Pasadena, CA 91109

*AT&T Bell Laboratories, Murray Hill, NJ 07974

INTRODUCTION

Infrared (IR) detectors operating from mid IR wavelengths to very long wavelength IR (i.e., 3-18 μm) are of great interest for a variety of ground based and space basal applications such as night vision, early warning systems, navigation, flight control systems, weather monitoring, and astronomy (IR detectors are used in the focal plane of telescopes). In addition IR detectors in this spectral region can be used for pollution monitoring, as well as monitoring the relative humidity profiles and the distribution of different constituents in the atmosphere (e.g., O_3, CO, N_2O). This is due to the fact that most of the absorption lines of gas molecules lie in this IR spectral region. Some examples are monitoring the global atmospheric temperature profiles to the accuracy of one Kelvin and the depth to one kilometer (by measuring the temperature dependence of the absorption signatures of the carbon dioxide molecules), relative humidity profiles, and the distribution of minor constituents in the atmosphere, studies which are already being planned for NASA's Earth Observing System[1] (EOS). This spectral

region is also rich in information vital to the understanding of composi t ion, st ruct ure and the energy balance. of molecular clouds and star forming regions of our galaxy. Thus, there is great commercial, scientific and academic interest in IR detectors operating in this wavelength region.

It is customary to make IR detectors in this spectral span by utilizing the interband absorption of narrow band gap semiconductors (e.g., InSb, $Hg_{1-x}Cd_xTe$). Fig. 1 shows the schematic band diagram of a conventional intrinsic detector which involves interband absorption. 1 R radiat ion is absorbed by the photosen sit ive material when an incoming photon has sufficient energy E (1> hv, where h is the. Planck's constant and v is the frequency of the incoming photon) to photoexcite an elect ron from the. valence band to the conduction band. In a detector structure these photoexcited carr iers are col lected by applying an electric fiel d, thereby produci ng a photocurr ent or a photovoltage. Since the absorbed photon ener gy is greater than the. energy of the band gap E_g, both electrons and the holes are created, thus, the semiconductor dots not need to be doped (these. detectors arc. called intrinsic detectors). I arge two di mensional arrays of lnSb (512x512 pixels) and $Hg_{1-x}Cd_xTe$ (128x 128 pixels) detectors have already been demonstrated up to cut off wavelengths of 5 μ m and 11 μm respect ivel y. in InSb, since the band gap is fixed, these detectors cannot be operated at longer wavelengths. on the other hand, $Hg_{1-x}Cd_xTe$ can made into narrow band gap materials by varying the alloy composition. 1 lowever, the long wavelength large 1 $Hg_{1-x}Cd_xTe$ arrays arc high] y non uni form in composition and doping (thus large nonuni formit ies in sped t-al response and sensitivit y). Further more, there are large nu mbers of trap centers throughout the. band gap and charged surface states (thus higher 1/f noise) which produce substantial ant] detrimental parasitic currents. in addition, such narrow band gap materials are more di fficult to grow and process into devices compared to wide

band gap semiconductors (thus low yield and high cost) [2]. These difficulties motivate the exploration of utilizing the *artificial* ***low effective*** band gap structures made of wide band gap semiconductors such as GaAs (see Fig. 2) which are easy to grow and process into devices. The basic advantages of the GaAs based quantum well infrared photodetectors (QWIPs), namely the highly mature GaAs growth and processing technologies, become more important at longer wavelengths where the narrow band gap materials becomes more difficult to work with.

The possibility of using $GaAs/Al_xGa_{1-x}As$ multi quantum well (MQW) structures to detect IR radiation was first suggested by Leo Esaki *et al.*[3] at the IBM Thomas J. Watson Research Center. The idea of using MQW structures to detect IR radiation can be understood by the basic principles of quantum mechanics. The quantum well is equivalent to the well known *particle in a* ***box*** problem in quantum mechanics, which can be solved by the time independent Schrodinger equation. The solutions of this problem are the Eigenvalues that define the energy levels inside the well in which the particle is confined (see Fig. 2). The positions of the energy levels are primarily determined by the well dimensions (height and width). Therefore, as shown in Fig. 3, by *tailoring* the quantum well structure, the separation between the allowed energy levels can be adjusted so that the IR photons can induce an intersubband transition between the ground state and the first excited state. The lattice matched $GaAs/Al_xGa_{1-x}As$ (where x is the molar ratio between Al and Ga) materials system is a good candidate in which to create such a potential well, since the band gap of $Al_xGa_{1-x}As$ is higher than that of the GaAs and can be changed continuously by varying, x (and hence the depth of the well or height of the barrier). Carriers (electrons for n-type material and holes for p-type material) can be introduced by doping, the GaAs well. These carriers will occupy the ground state of the quantum wells at low temperatures.

The first experimental investigation of MQW structure to detect 1 R radiation was carried out by John Smith *et al.* [4] at the California Institute of Technology, and theoretically analyzed by 1 Darryl Coon *et al.*[5] at the University of Pittsburgh. The first experimental observation of the strong intersubband absorption within the quantum wells in the conduction band was performed by 1 awrence West *et al.*[6] al Stanford University, and the first QWIP was demonstrated by Barry 1 mine *et al.* [7] at the AT&T Bell 1 aboratories. This first QWI P was based on intersubband transition between two bound quantum wC]] states (i.e., ground state and the first excited state are inside the well). The intersubband absorption excites an electron from the ground state to the. first excited state, where. it can tunnel out to the. continuum (continuous energy levels above the quantum well) in the presence of an external electric field, thereby producing a photocurrent as shown in Fig. 4.

in addition to the photocurrent, all detectors including QWIPs produce a parasitic current which is a called dark current, and this must be minimized to achieve high performance.. in QWIPs, the. dark current originates from three different mechanisms as shown in 1 ig. S. The dark current arising from the first process is due to quantum mechanical tunneling from well to well through the $Al_xGa_{1-x}As$ bar-rim-s (sequential tunneling). This process is independent of temperature. Sequential tunneling dominates the dark current at very low temperatures (<30 K). The second mechanism is thermally assisted tunneling which involves a thermal excitation and tunneling through the tip of the barrier into the continuum energy levels. This process governs the dark current at medium temperatures. The third mechanism is classical thermionic emission and dominates the dark current at higher temperatures (>45 K). Fig. 6 shows the dark cw-rent and the photocurrent of typical 15 μm QWI 1' at various temperatures

(photocurrent is independent of temperature). At higher temperatures the last mechanism is the major source of dark current, and the thermal generation rate is determined by the lifetime of the carriers and the well doping density. In this case, the carrier lifetime will determined by the thickness of the $Al_xGa_{1-x}As$ barriers as described by Emmanuel Rosencher *et al.* [8] at the Thomson-CSF Research Laboratory, France. The dependence of the dark current (and hence the detector performance) on doping density was analyzed by Sarath Gunapala *et al.*[9] at the AT&T Bell Laboratories. In particular they have found that the dark current can be reduced by many orders of magnitude by lowering the well doping, density, without significantly reducing, the performance of the detectors.

By reducing the quantum well width it is possible to *push* the second bound state (first excited state) into the continuum resulting in a strong *bound-to-continuum* intersubband absorption as shown in Fig. 4. The major advantage of the bound-to-continuum QWIP is that the photoexcited electron can escape from the quantum well to the continuum transport states without being required to tunnel through the barrier, as shown in Fig. 4. As a result, the bias required to efficiently collect the photoelectrons can be reduced dramatically, thereby lowering the dark current, Due to the fact that the photoelectrons do not have to tunnel through the barriers, the $Al_xGa_{1-x}As$ barrier thickness of bound-to-continuum QWIP can now be increased without reducing the photoelectron collection efficiency. in addition, increasing the barrier width from a few hundred Å to 500 Å can reduce the ground state sequential tunneling, by an order of magnitude. By making use of these improvements, Barry Levine *et al.*[7] at the AT&T Bell Laboratories successfully demonstrated the first bound-to-continuum QWIP operating at 10 μm with a dramatic improvement in the performance. Due to this high performance and the excellent uniformity of GaAs based QWIPs, several groups have

demonstrated large (two dimensional array of 128x128, 256x256, and **5 12x512** pixels) imaging arrays-l~lo-11 up to a cut off wavelength of 10 µm.

VERY LONG WAVELENGTH QWIP

Most of the QWIP work described in the previous sections has concentrated on the 8-10 µm spectral band, alt hough peak wavelengths as short as $\lambda_p = 2.7$ µm have been demonstrated. The design of QWIPs operating in the 8 - 10 µ m atmospheric window typically consists of 40 Å wide GaAs quantum wells and 500 Å thick $Al_xGa_{1-x}As$ barriers with x ≈ **0.3.** in order to tailor the QWI P response to the very long wavelength spectral region ($\lambda_c > 12$ µm) the barrier height should be lowered; however, in addition to lowering the barrier height, the quantum well width must be widened in order to lower the photoexcited continuum state. closer to the top of the. barrier. By doing this very long wavelength IR (VI .WIR) QWIPs up to a cut off wavelength of 19 µm have been demonstrated by Avigdor Zussman *et al.*[12] at the AT&T Bell Laboratories.

In order to optimize the performance of V] .WIR QWIPs Gabby Sarusi *et al.*[13] at the AT&T Bell Laboratories have ut ilized the *bound-to-quasicontinuum* intersubband absorption (occurring when the first excite.(i state is in resonance with the top of the barrier). 'l'his transition maximizes the intersubband absorption, while maintaining the excellent electron transport. The device struct ure of a QWI P operat ing at $\lambda_p = 15$ µm typically consists of 65 - 70 Å wide GaAs quantum wells and 600 Å thick $Al_xGa_{1-x}As$ barriers with x ≈ **0.15.** These structures arc. grown by the technique of molecular beam epitaxy (M BE), and consist of 50 periods of quantum wells and barriers, sandwiched between ().5 µm top and 1 µ m bottom Si doped $N_D = 1 \times 10^{18}$ cm^{-3} contact layers. The quantum well doping of 8 - 10 µm QWIPs is usually $N_D = 1 \times 10^{18}$ cm^{-3}. However, in

order to lower the Fermi level (E_F) of the carriers, in these very long wavelength (λ_c = 16.5 pm) QWIPs, so as not to be too large a fraction of the cutoff energy $E_c = hc/\lambda_c$, and to reduce the thermal generation rate, well doping density has been substantially reduced to $N_D = \sim .x10^{17}$ cm^{-3}.

LIGHT COUPLING

QWIPs do not absorb radiation incident normal to the surface since the light polarization must have an electric field component normal to the superlattice (growth direction) to be absorbed by the confined carriers. As shown in Fig. 7, when the incoming light contains no polarization component along the growth direction, the matrix element of the interaction vanishes (i.e., $\vec{\varepsilon}.\vec{p}_z = 0$ where $\vec{\varepsilon}$ is the polarization and $\vec{p}_z$ is the momentum along z direction). As a consequence, these detectors have to be illuminated through a 45° polished facet [7] (see Fig. 8(a)). Clearly, this illumination scheme limits the configuration of detectors to linear arrays and single elements. For imaging, it is necessary to be able to couple light uniformly to two dimensional arrays of these detectors. Keith Goosen *et al.*[14] at Princeton University have demonstrated efficient light coupling to a QWIPs using linear gratings which removed the light coupling limitations and made two dimensional QWIP imaging arrays feasible (see Fig. 8(b)). These line gratings were made of metal on top of each detector or groove etched through a cap layer on top of the quantum well structure. These gratings deflect the incoming light away from the direction normal to the surface, enabling intersubband absorption. The normal incidence light coupling efficiency of line gratings is comparable to the light coupling efficiency of a 45° polished facet illumination scheme and yields an quantum efficiency (the fraction of the incident photons effective in producing the emitted electrons) of about 10-20% (for QWIPs having 50 periods and

$N_D = 1x10^{18} cm^{-3}$). This relatively low quantum efficiency is due to the poor light coupling efficiency and the fact that only one polarization of the light is absorbed. in order to maintain high absorption and thus high quantum efficiency, the quantum well doping density must be kept very high, leading to a higher dark current. In order to further increase the quantum efficiency without increasing, the dark current, Jan Anderson *et al.*[15] at the industrial Microelectronics Center, Sweden, developed the cross grating (or two dimensional grating) for QWIPs operating at the 8 - 10 μm spectral range. in this case the periodicity of the grating, is repeated in both directions, leading to the absorption of both polarizations of incident 1 R light. The addition of optical cavity results in two optical passes through the MQW structure before the light is diffracted out through the. substrate, as shown in Fig. 8(c).

Many more passes of 1 R light, and significantly higher absorption, can be achieved with a randomly roughened reflecting surface, as shown in Fig. 9(a). Gabby Sarusi *et al.*[16] at the AT&T Bell Laboratories have shown experimentally that by careful design of surface texture randomization, efficient light trapping can be obtained. They demonstrated nearly an order of magnitude enhancement in responsivity compared to 45° illumination geometry. The random structure on top of the detector prevents the light from being diffracted normally backward after the second bounce as happens in the Case of cross-grating (see Fig. 8(c)). After each bounce, light is scattered at a different random angle and the only chance for light to escape out of the detector is when it is reflected towards the surface within the critical angle of the normal. For the GaAs/air interface this angle. is about 17°, defining a very narrow escape cone for the trapped light. Some considerations have been taken into account when designing such random scatters to reduce the probability of light being diffracted into the escape cone. The reflector was designed with three levels of scattering sLn-faces located at quarter

wavelength separations, as shown in Figs. 9(b) and 9(d). As shown in Fig 9(b) and 9(c) these scattering centers were arranged in cells to prevent clustering of the scattering centers, having the same dimension as the light wavelength in GaAs. The combined area of the top unetched level and the bottom level ($\lambda/2$ deep) arc. $U^2/2$ (where U^2 is the area of a unit cell as shown in Fig. 9(b)). The area of the intermediate level ($\lambda/4$ deep) is also $U^2/2$. These reflecting areas and depths were chosen such that the normally reflected light intensities from two adjacent surfaces are equal and 180° out of phase, thus maxi mizing the destructive interference at normal reflection (and hence lower the light leakage. through the escape cone). These scattering centers were organized randomly inside the cell as shown in Fig. 9(c). This random structure was fabricated on the. detectors by using standard photolithography and selective dry etching. The advantage of the photolithographic process over a completel y random proms is the ability to accuratel y cent rol the feat ure size at id to pre.serve. the. pixel to pixel uniform it y which is a prerequisite for **high** sensitivity imaging focal plane arrays. It is clearly evident from the experi ments that maxi mum respon sivit y is obtained when the unit cell size is equal to the wavelength of the QW11) maximum response. When this condition is met, light scattering becomes very efficient. I f the unit cell is larger than the. wavelength of the I R radiation (in GaAs), the number of scat tering centers on the detector surface will decrease and the light is scattered less e fficiently. On the. other hand, if the unit cell size is smal ler than the wavelength (in GaA s), the scat tering surface becomes effectively smoother, and as a consequence scattering efficiency again decreases. Naturally, thinning down the substrate enables more bounces of light and therefore higher responsivity. One of the main di fferences bet ween the. effect of the cross grating and the random reflector is the shape of the responsivity curve; unlike the cross grating, the random reflector has little impact on the bandwidth of the response curve since the scat tering efficiency of the random reflector is significantly less wavelength dependent

than for the regular grating. Therefore, for the QWIPs with random reflectors, the integrated responsivit y is enhanced by nearly the same amount as the peak responsivit y.

DETECTOR AND ARRAY PERFORMANCE

1 igures of merit such as responsivity and detectivity are commonl y used to compare the performance of detectors. Responsivity is the ratio of the signal current to the incident radiation power on the. detector. I ig. 10 shows typical photoresponse curves of very long wavelength bound-to-con tinuum QWI Ps at temperat ure T= 55 K. The absorption and photoresponse curves of bound-to-continuum QWIPs arc. much broader than those of the bound-to-bound QWIPs. 1)etectivity (D^*) is the signal to noise ratio nor malized to unit area and unit bandwidth. The primary noise source in QWIPs is the shot noi sc produced by the dark current. Therefore, unlike the narrow band gap detect ors, in which the noise is domi nated by temperat ure independent processes at low temperat ures, QWIP performance can be further i mproved by cooling to cryogenic temperatures, as shown in 1 ig. 11.

As can be seen from I ig. 12 rapid progress has been made in the performance (detectivity) of very long wavelength QWIPs, starting with bound-to-bound QWIPs which had relat i vel y poor sensitivit y, and cul mi nat ing in high performance. bound-to quasicontinuum QWIPs with random reflectors. 'l'he achieved detectivit ics are more than sufficient to demonstrate. large two dimensional imaging arrays (128x128 or larger) at very long wavelength, which is presentl y not possible with intrinsic narrow band gap detectors. I ig. 13 shows a pict ure of a 128x 12.8 QWIP two dimensional imaging array produced by the. Jet l'repulsion 1 aboratory, which has a peak rcspon sivit y at 15 μm. I ig. 14 present an expanded image showing, the random

reflectors on the pixels (single elements) of this imaging array. Due to the pixel-to-pixel nonuniformities, the detectivity of a single pixel is not sufficient to describe the performance of a large imaging array. Noise. induced by nonuniformity y has to be taken into account for complete evaluat ion. '1 'his point has been di scussed in detail by Freeman Shepherd *et al.*[17] at the U.S. Air 1 'orce Rome 1 aboratories for the case of PtSi infrared focal plane arra ys which have low response, but very high uni fermi t y. The gene.ral figure of merit to describe the perfor mance of a large imaging array is the noise equivalent temperat ure di fference NEΔT, which i ncludes t he spatial mist originating, from pixel-to-pixel nonuniform i tics. NEΔT is the minimum temperature difference across the. target that would produce a signal - to-noi se ratio of unity. Due to superior material quality and the high uniformity associated with the GaAs/$Al_xGa_{1-x}As$ materials system, an-a ys of very long wavelength QWI 1' with very low N EΔT wi ll be a reality in the near future.

NEW MATERI Al .S SYSTEM

A ll t he VI .WI R QWIPs which have been di scussed thus far arc based on the *lattice matched* GaAs/$Al_xGa_{1-x}As$ materials system. However, it is i nteresti ng to consider GaAs as the *barrier* material since the transport in binary GaAs is expected to be superior to that of a ternary alloy such as $Al_xGa_{1-x}As$, as was previous] y found to be the case in the $In_{0.53}Ga_{0.47}As$/InP binary barrier structures [18]. To achieve this, Sarath Gunapala *et al.*[19] at the. Jet Propulsion 1 abor atory have used the lower band gap non-lat [ice matched alloy $In_xGa_{1-x}As$ as well mate.rial together with GaAs barriers. 'l'his heterobarrier system is also well suited for very kmg-wavelength ($\lambda > 14$ pm) QWIPs.

These non-l attice matched GaAs/$In_{0.2}Ga_{0.8}As$ QWIPs were grown by MBE on a semi - insulating GaAs substrate.. The detector structure consi sted of 0.5 μ m GaAs top

and 1 μm bottom contact layers Si doped with 1×10^{17} cm^{-3}, and 10 sets of doped (doping density $N_D = 5 \times 10^{17}$ cm^{-3}) $In_{0.2}Ga_{0.8}As$ quantum wells of well width L_w, separated by nine 60 nm undoped GaAs barriers. In addition, all of these structures contain 60 nm thick GaAs spacer layers between the quantum wells and the top and bottom contact layers. Despite the 1.2% lattice mismatch between $In_{0.2}Ga_{0.8}As$ and GaAs, excellent quality non-lattice matched GaAs/$In_{0.2}Ga_{0.8}As$ QWIP structure have been grown. [15]

The responsivity of this $In_{0.2}Ga_{0.8}As$/GaAs detector peaks at 16.7 μm and the peak responsivity is 790 mA/W at bias $V_B = 300$ mV. These results also indicate excellent electron transport in this device structure due to the high mobility binary GaAs barriers. This very long-wavelength ($\lambda_c = 18$ μm) $In_xGa_{1-x}As$/GaAs QWIP had a detectivity D^* of 1.8×10^{10} cm√Hz/W at $\lambda_p = 16.7$ μm operating at T = 40 K. The large responsivity and detectivity D^* values are comparable to those achieved with the lattice matched GaAs/$Al_xGa_{1-x}As$ materials system, and hence further study seems warranted.

SUMMARY

Exceptionally rapid progress has been made in the development of very long wavelength QWIPs, since they were first experimentally demonstrated only a few years ago. Now it is possible for VLWIR QWIPs to achieve excellent performance (e.g., detectivities as high as D^* of 8×10^{10} cm√Hz/W at 55 K for 15 μm QWIP). This operating temperature can be easily achieved by single stage Stirling coolers. Fig. 12 shows the evolution of high sensitivity very long wavelength QWIPs. A mission currently under development at the Jet Propulsion Laboratory is the Atmospheric IR Sounder (AIRS). This mission will monitor the 3-15 μm infrared region to obtain the

at mospheric temperat ure profile and ot her atmospheric properties. 1 Due to the. high internal i mpedance, low 1/f noise, high radiation hardness, low cost (see Fig. 15), easy h ybridization to readout electronics, and high uniformity of QWI P, it is a potential candidate for the VI.WIR focal plane. arrays of AIRS where the fabrication of $Hg_{1-x}Cd_xTe$ detector arrays becomes increasingl y difficult.

ACKNOWLEDGMENTS

The research described in this paper was performed partly by the Center for Space Microelectronics Technology, Jet Propulsion I abm-story, California Institute o f Technology, and was jointly sponsored by the Ballistic Missile Defense Organization/In novative Science and Technology office, and the National Aeronautics and Space Administrat ion, Office of Advanced Concepts and Technolog y.

REFERENCES

1. M. '1'. Chahine, Proceedings of Innovative 1 ong Wavelength Infrared Detector Workshop, Pasadena, California, April 24-26, 1990.
2. B. F. Levine, Appl. Phys. I ett., 56,2354 (1990).
3. L. Esaki and }1. Sakaki, IBM Tech. Disc. Bull. 20,2456 (1977).
4. J. S. Smith, L. C. Chiu, S. Margalit, A. Yariv, and A. Y. Cho, J. Vat. Sci. Technol. B 1, 376 (1983).
5. 1>.11. Coon and R. P. G. Karunasiri, Appl. Phys. I ett. 4S, 649 (1984).
6. J.. C. West and S. J. Eglash, Appl. Phys. 1 ett. 46, 1156 (1985).
7. B. F. 1 mine, J. Appl. Phys. 74, R 1 (1993).
8. 1 L. Rose.nchcr, F. I uc, P. Bois, J. Nagle, and Y. Cordier, Appl. Ph ys. I ett., 63,3312, (1993).

9. S. D. Gunapala, 13.1'.1 .evine, L. Pfeiffer, and K. West, J. Appl. Phys. **69**, 6517 (1991).

10. I. J. Kozlowski, G. M. Williams, G. J. Sullivan, C. W, Farley, R. J. Andersson, J. Chen, 1). T. Cheung, w. E. Tennant, and R. E. DeWames, IEEE Trans. Electron. Devices **ED-38**, 1 124 (1991).

11. W. A. Beck, 'I'. S. Faska, J. W. Little, J. Albritton, and M. Sensiper, Second International Symposium on 2-20 μm Wavelength Infrared Detectors and Arrays: Physics and Applications, October 10-12, 1994, Miami Beach, Florida.

12. A. Zussman, B. F. Levine, J. M. Kuo, and J. de Jong, J. Appl. Phys. 7O, 51O1 (1991).

13. G. Sarusi, S. D. Gunapala, J. S. Park, and B. F. Levine, to be published in J. Appl. Phys. November 1 (1994).

14. K. W. Goosen and S. A. Lyon, Appl. Phys. 1 ett. 47, 1257 (1985).

15. J. Y. Andersson, 1,. Lundqvist, and Z. F. Paska, Appl. Phys. Lett. **58**, 2264 (1991).

16. G. Sarusi, B. F. Levine, S. J. Pearton, K. M. S. V. Bandara, and R. E. Leibenguth, Appl. Phys. 1 ett. 64,960 (1994).

17. 1 '. D. Shepherd, in Infrared Detectors and Arrays, SPIE Vol. 930 (SPIE, Orlando, Florida, 1988), p.2.

1 8. S. D. Gunapala, B. F. Levine, D. Ritter, R. A. Hamm, and M. B. Panish, Appl. Phys. Lett. 58,2.024 (1991).

19. S. D. Gunapala, K, M. S. V. Bandara, 11. 1:.1 evine, G. Sarusi, J. S. Park, T. L. Lin, W. 'I'. Pike, and J. K. Liu, J Appl. Phys. Lett. 64,3431 (1994).

FIGURE CAPTIONS

1 ig. 1 Band diagram of conventional intrinsic infrared photodetector.

J ig. 2. Schematic band diagram of a quantum well. Intersubband absorption can take place between the energy levels of a quantum well associated with the conduction band or the valence band.

1 ig. 3 Calculated peak wavelength (λ_p) of bound-to-con tinuum QWI I' as a function of $Al_xGa_{1-x}As$ barrier composition (x) foi various quantum well widths.

Fig. 4 A typical conduction-band diagram of very long wavelength bound-to-continuum quantum well infrared photodetector.

Fig. 5 Dark current mechanisms of QWIP.

Fig. 6 Dark current and the 300 K window photocurrent of a VLWIR QWIP (λ_p= 15 μm) at various temperatures. Photocurrent is independent of the temperature.

Fig. 7 QWIPs (with no light coupling scheme) do not absorb normal incident IR light since there is no light polarization component along the quantum well direction (growth direction).

Fig. 8 Different light coupling mechanisms used in QWIPs. (a) 45° polished facet, (b) linear or two dimensional gratings on each detector, and (c) gratings with optical cavity.

Fig. 9 (a) Schematic side view of a thin QWIP pixel with a random reflector. Ideally all the radiation is trapped except for a small fraction which escape through the escape

cone (defined by critical angle Θ_c), (b) top view of the unit cell of the scattering surface (arrows indicate the 16 random possibilities), (c) top view of the. one of the 16 possibilities, (d) side view of the unit cell.

Fig. 10 Typical photoresponse curves of bound-to-continuum VLWIR QWIPs at temperature T = 55 K.

Fig. 11 Detectivity of VLWIR QWIP as a function of temperature. Unlike the narrow band gap detectors, detectivity increases with decreasing temperature.

Fig. 12 Evolution of the performance of very long wavelength QWIP.

Fig. 13 Picture of the first ***15*** μm ***128x128*** QWIP focal plane array.

Fig. 14 Random reflectors on pixels (38x38 μm^2) of QWIP focal plane army. The random reflectors increase the light coupling efficiency by factor of eight when the substrate thin down to - 25 μm

Fig. 15 Thirty five 128x128 QWIP focal plane arrays on 3 in. GaAs wafer.

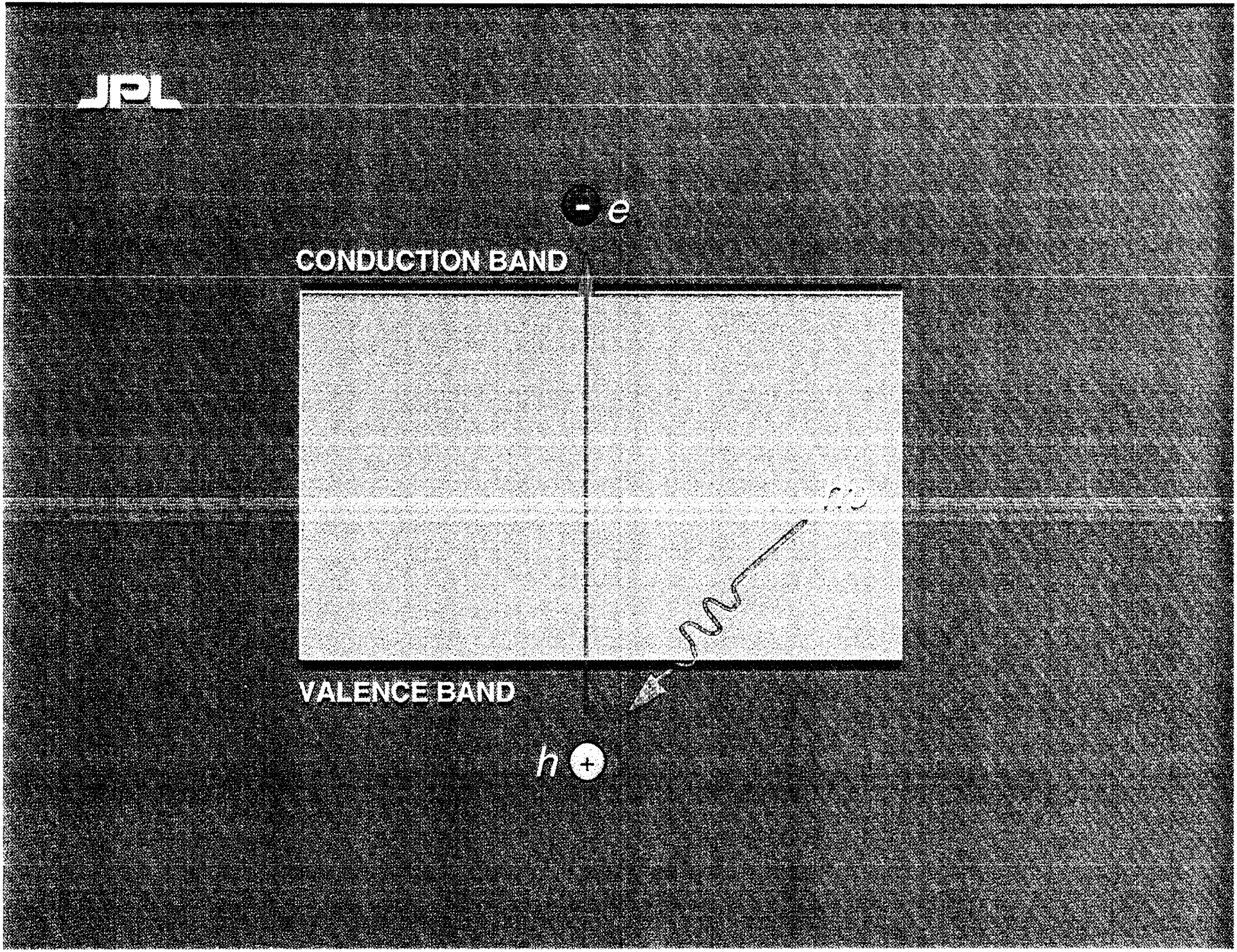
JPL
e
CONDUCTION BAND
VALENCE BAND
h

JPL
CONDUCTION BAND
ENERGY (eV)
VALENCE BAND

JPL
PEAK WAVELENGTH λ_p (μm)
20
18
16
14
12
10
0
0.12
0.16
0.20
0.24
Al COMPOSITION x

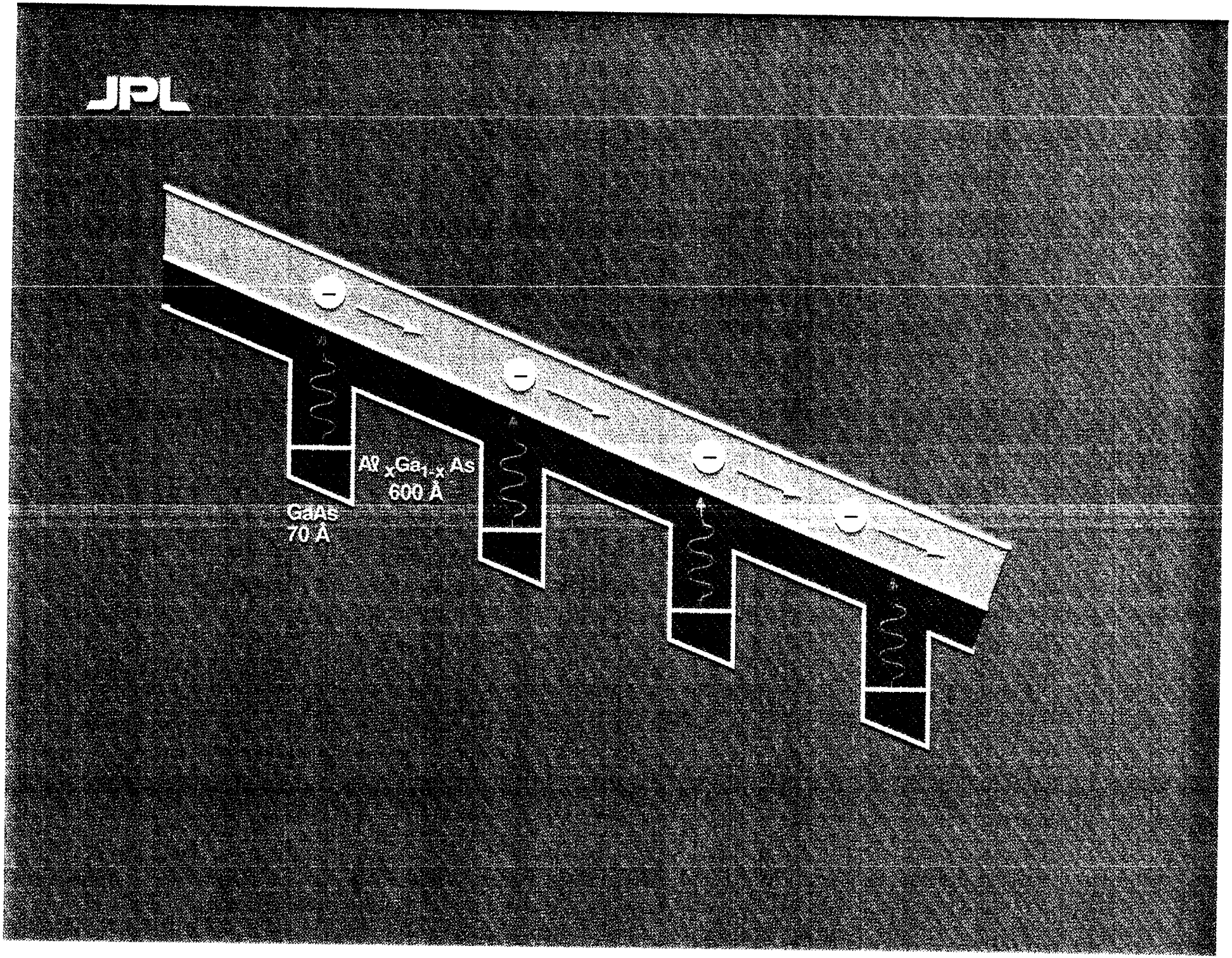
JPL
$Al_xGa_{1-x}As$
600 Å
GaAs
70 Å

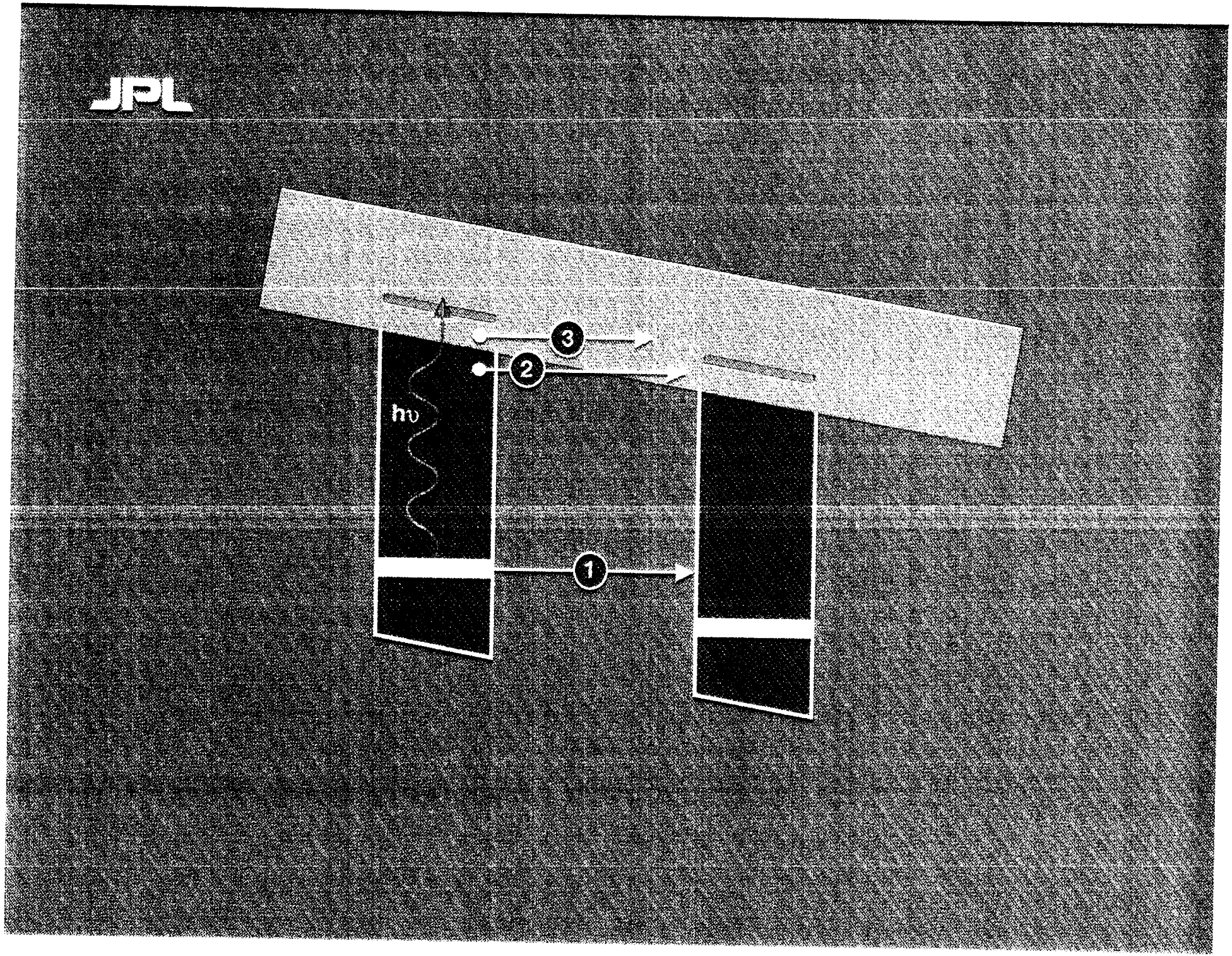
JPL
hυ
3
2
1

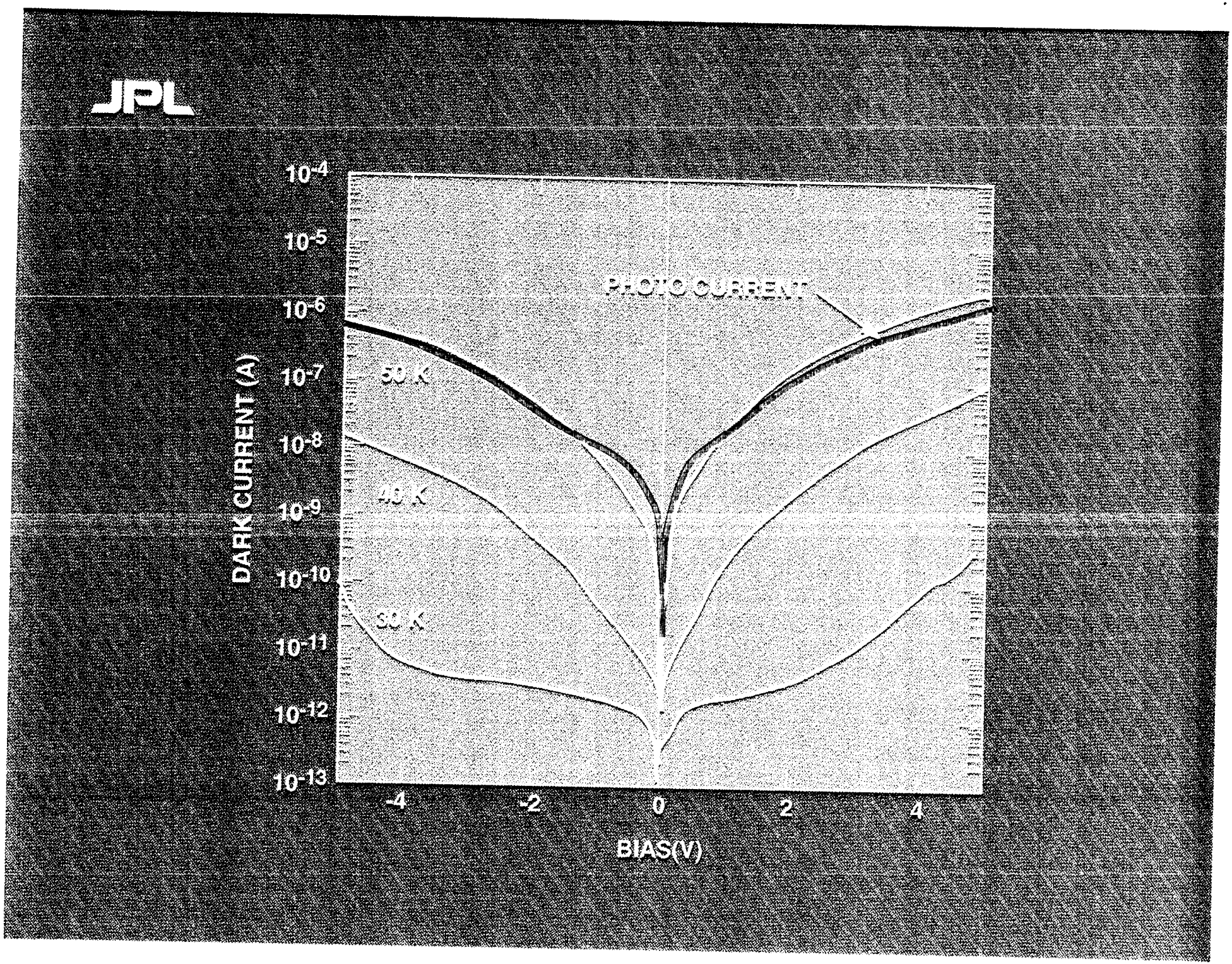
JPL
DARK CURRENT (A)
10-4
10-5
10-6
10-7
10-8
10-9
10-10
10-11
10-12
10-13
PHOTO CURRENT
50 K
40 K
30 K
-4
-2
0
2
4
BIAS(V)

JPL

JPL

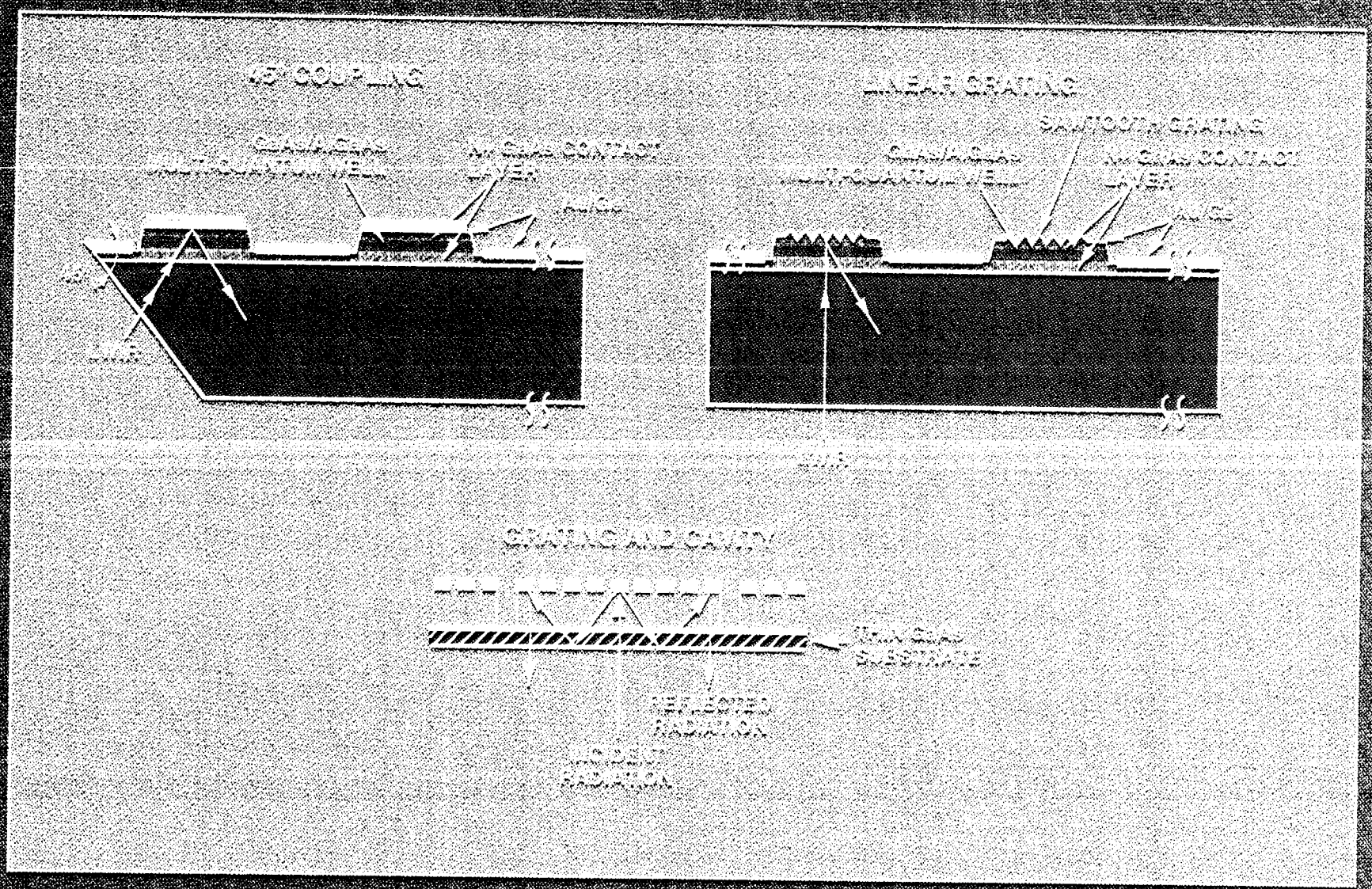

JPL

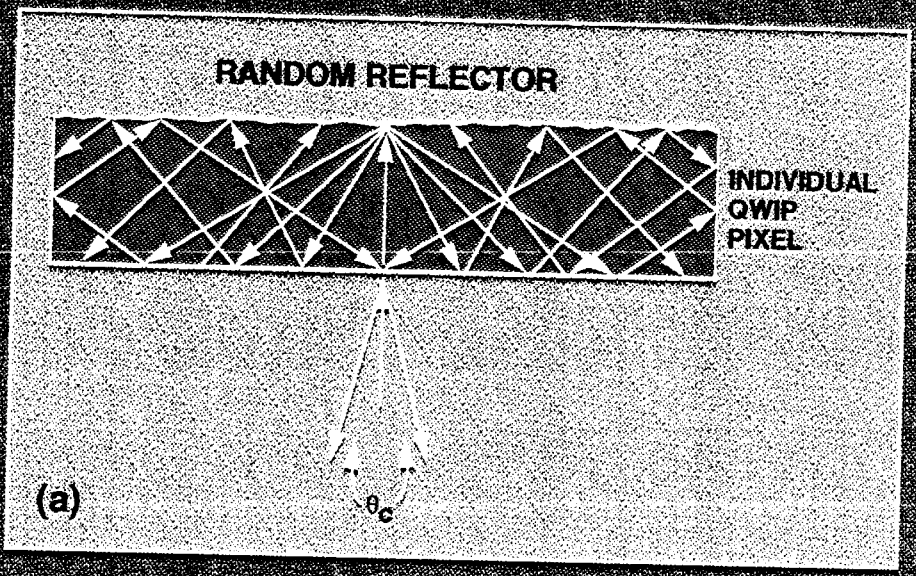
RANDOM REFLECTOR
INDIVIDUAL
QWIP
PIXEL
θ_c
(a)

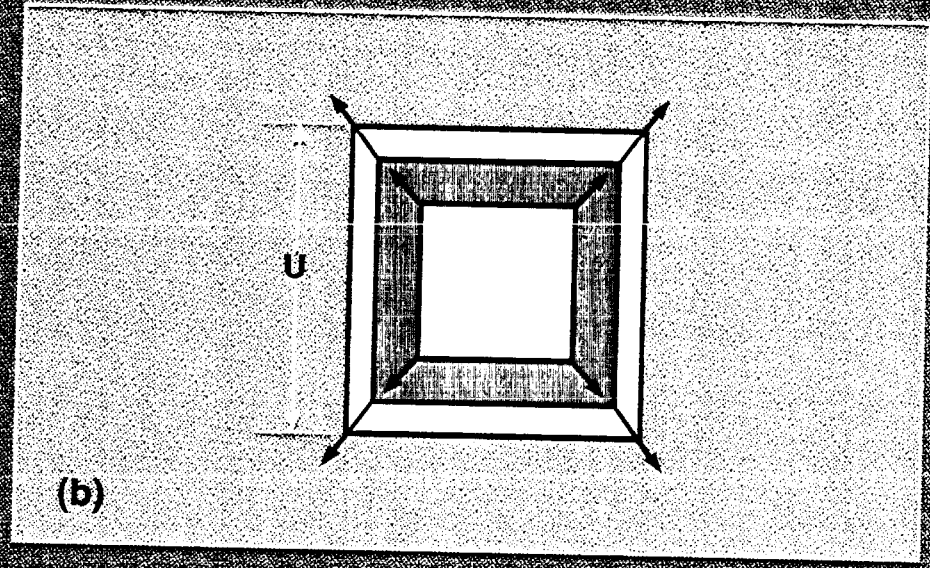
U
(b)

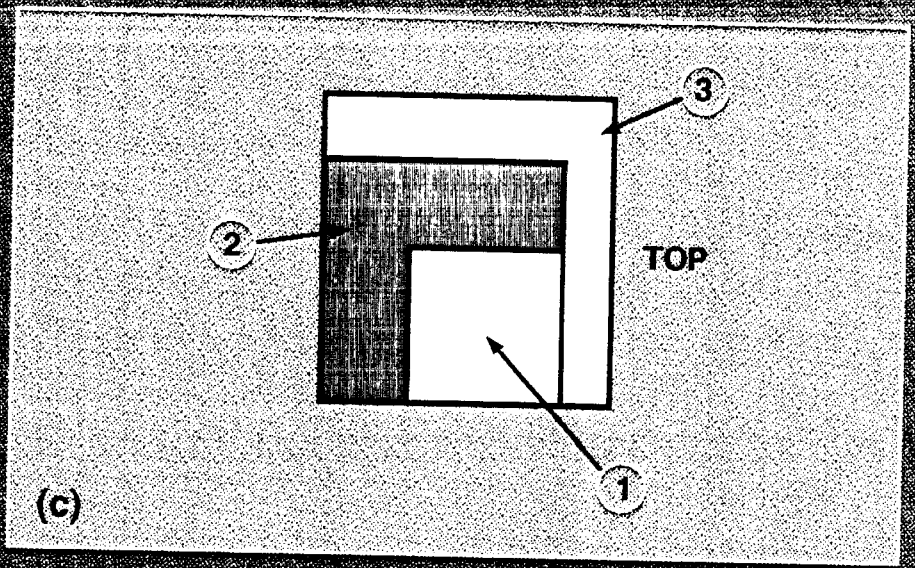
3
2
TOP
1
(c)

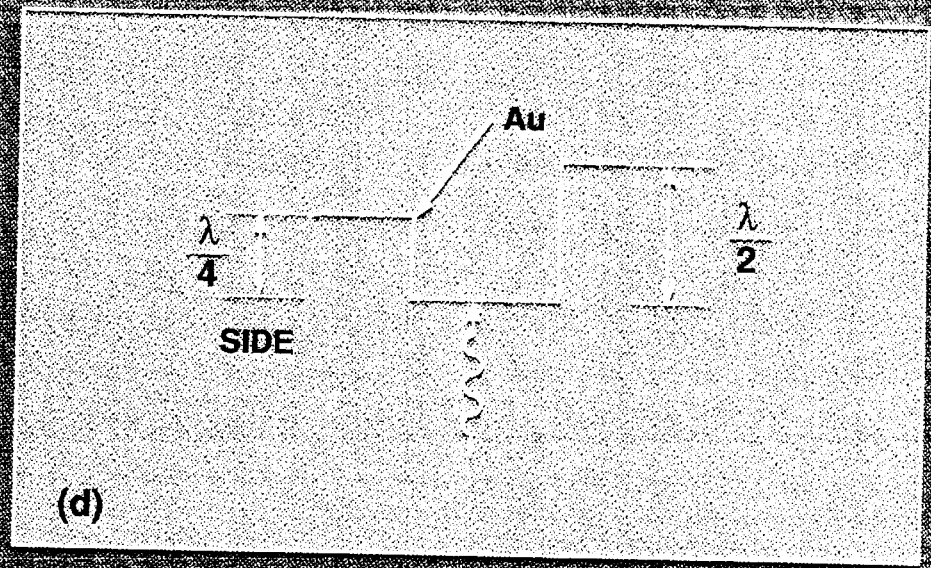
Au
$\frac{\lambda}{4}$
$\frac{\lambda}{2}$
SIDE
(d)

JPL

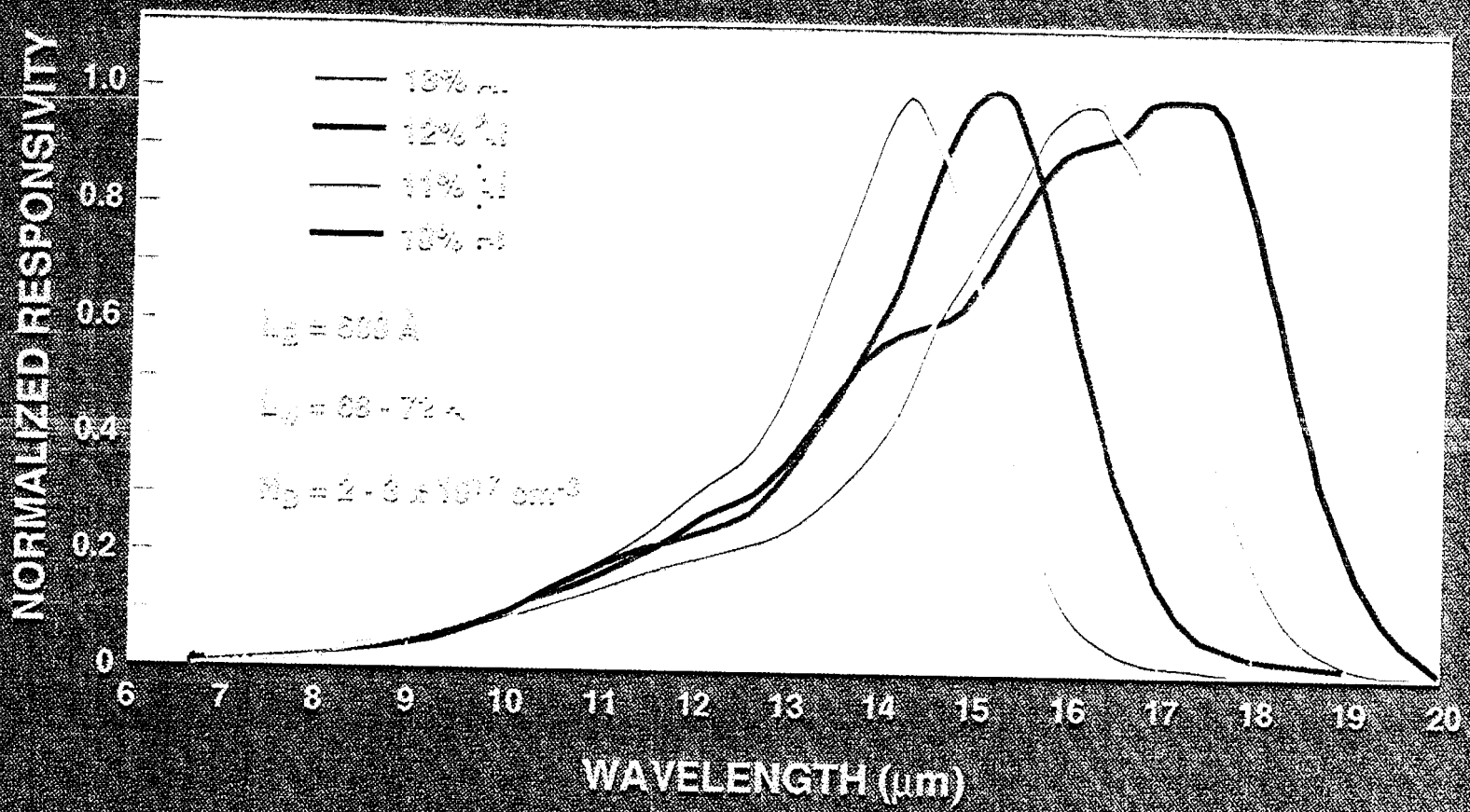
NORMALIZED RESPONSIVITY
1.0
0.8
0.6
0.4
0.2
0
6
7
8
9
10
11
12
13
14
15
16
17
18
19
20
WAVELENGTH (μm)

JPL
DETECTIVITY, D* (cmVHz/W)
10^{14}
10^{13}
10^{12}
10^{11}
10^{10}
30
40
50
60
TEMPERATURE (K)

JPL D* NORMALIZED FOR λ_c = 15.4 μm, T = 5.5K

QWIP